Ding and Li *SpringerPlus (2016)5:1490*
DOI 10.1186/s40064-016-3105-5

SpringerPlus

RESEARCH Open Access

Interface crack between different orthotropic media under uniform heat flow

Sheng-Hu Ding* and Xing Li

*Correspondence:
dshsjtu2009@163.com
School of Mathematics and Computer Science, Ningxia University, Yinchuan 750021, China

Abstract

In this paper, plane thermo-elastic solutions are presented for the problem of a crack in two bonded homogeneous orthotropic media with a graded interfacial zone. The graded interfacial zone is treated as a nonhomogeneous interlayer having spatially varying thermo-elastic moduli between dissimilar, homogeneous orthotropic half-planes, which is assumed to vary exponentially in the direction perpendicular to the crack surface. Using singular integral equation method, the mixed boundary value conditions with respect to the temperature field and those with respect to the stress field are reduced to a system of singular integral equations and solved numerically. Numerical results are obtained to show the influence of non-homogeneity parameters of the material thermo-elastic properties, the orthotropy parameters and the dimensionless thermal resistance on the temperature distribution and the thermal stress intensity factors.

Keywords: Functionally graded orthotropic media, Interface zone, Crack, Singular integral equation, Stress intensity factors

Background

Functionally graded materials (FGMs) are designed as the special materials which have changed micro-structure and mechanical/thermal properties in the space to meet the required functional performance (Niino et al. 1987; Suresh and Mortensen 1998). The advantages of FGMs are that the magnitude of residual and thermal stresses can be reduced, and the bonding strength and fracture toughness of such materials can be improved. From both the phenomenological and mechanistic viewpoints, the tailoring capability to produce gradual changes of thermo-physical properties in the spatial domain is the key point for the impressive progress in the areas of functionally graded materials (Miyamoto et al. 1999).

By introducing the concept of the FGMs, extensive research on all aspects of fracture of isotropic and orthotropic FGMs under mechanical or thermal loads has been considered (Choi et al. 1998; Choi 2003; Wang et al. 2004; El-Borgi and Hidri 2006; Han and Wang 2006; Cheng et al. 2010; Ding and Li 2014; Kim and Paulino 2002; Dag 2006; Zhou et al. 2007). By considering changes in both elastic and thermal properties, Jin and Noda (1991) studied the transient thermo-elastic problems of functionally graded material with a crack. Fujimoto and Noda (2001) investigated the thermal cracking under a

transient-temperature field in a ceramic/metal functionally graded plate. In addition, assuming the surfaces of the crack are insulated, thermal stresses around a crack in the interfacial layer between two dissimilar elastic half-planes are studied by Itou (2004). With the introduction of the thermal resistance concept, the thermal stress intensity factors for the interface crack between functionally graded layered structures under the thermal loading are investigated by Ding and Li (2015). Zhou and Lee (2011) studied the thermal fracture problem of a functionally graded coating-substrate structure of finite thickness with a partially insulated interface crack subjected to thermal–mechanical supply. Chen (2005) obtained the thermal stress intensity factors (TSIFS) of a graded orthotropic coating-substrate structure with an interface crack. Zhou et al. (2010) considered the thermal response of an orthotropic functionally graded coating-substrate structure with a partially insulated interface crack.

Using mesh-free model, Dai et al. (2005) studied the active shape control as well as the dynamic response repression of the functionally graded material (FGM) plate containing distributed piezoelectric sensors and actuators. Natarajan et al. (2011) considered the linear free flexural vibration of cracked functionally graded material plates by using the extended finite element method. Using extended finite element method, fatigue crack growth simulations of bi-material interfacial cracks have been considered under thermo-elastic loading (Pathak et al. 2013). Using element free Galerkin method, Pathak et al. (2014) studied quasi-static fatigue crack growth simulations of homogeneous and bi-material interfacial cracks under mechanical as well as thermo-elastic load.

Layered FGM structure are very import in practical engineering (Sofiyev and Avcar 2010; Sofiyev et al. 2012; Ding et al. 2014; Ding et al. 2015). The research of thermal elastic crack problem in layered structure is helpful for the design and application of functionally graded materials. This paper explores the thermal–mechanical response of layered and graded structures using the integral equation approach. The analytical results of the cracked layered material systems with the material properties in the graded coating varying as an exponential function has been obtained by using the integral transform technique. The surface of the crack is assumed to be part of the thermal insulation. The temperature distributions along the crack line are presented. The TSIFS under thermo-mechanical loadings are obtained, which is very important for the designing of layered orthotropic media.

Problem formulation

As shown in Fig. 1, the problem under consideration consists of a functionally graded orthotropic strip (FGOS) of thickness h bonded to two homogeneous semi-infinite orthotropic media with a partially insulated interface crack of length $2c$ along the x-axis is considered. The subscript $j(j = 1, 2, 3)$ indicates the FGOS and two semi-infinite orthotropic media respectively. The remaining thermo-mechanical properties depend on the y-coordinate only and are modeled by an exponential function

$$\left(k_x^{(1)}, k_y^{(1)}\right) = \left(k_x^{(2)}, k_y^{(2)}\right) \exp\left(\delta y / c\right) \tag{1}$$

$$\left(k_x^{(3)}, k_y^{(3)}\right) = \left(k_x^{(2)}, k_y^{(2)}\right) \exp\left(\delta h / c\right) \tag{2}$$

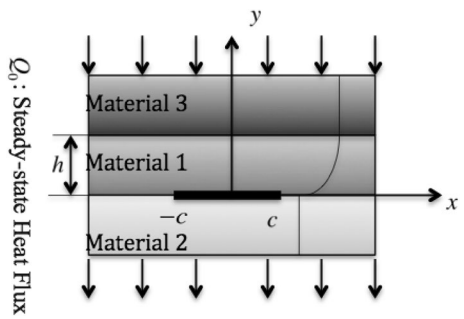

Fig. 1 Geometry of the layered orthotropic media under steady-state heat flows

where $k_x^{(2)}, k_y^{(2)}$ are the thermal conductivities for the homogeneous orthotropic substrate *II*, and δ is an arbitrary nonzero constant.

The temperature satisfies

$$\frac{\partial}{\partial x}\left(k_x^{(j)}\frac{\partial T_j}{\partial x}\right)+\frac{\partial}{\partial y}\left(k_y^{(j)}\frac{\partial T_j}{\partial y}\right)=0 \quad (j=1-3) \tag{3}$$

Substituting Eqs. (1) and (2) into the Eq. (3), the heat equation can be given by

$$k_{xy0}\frac{\partial^2 T_1}{\partial x^2}+\delta\frac{\partial T_1}{\partial y}+\frac{\partial^2 T_1}{\partial y^2}=0 \quad 0<y<h \tag{4}$$

$$k_{xy0}\frac{\partial^2 T_j}{\partial x^2}+\frac{\partial^2 T_j}{\partial y^2}=0 \quad (j=2,3) \tag{5}$$

where $k_{xy0}=k_x^{(2)}/k_y^{(2)}$.

The heat flux components are written as

$$\begin{aligned} k_3\frac{\partial T_1(x,y)}{\partial y}&=-Q_0, y\to+\infty, |x|<+\infty\\ k_2\frac{\partial T_2(x,y)}{\partial y}&=-Q_0, y\to-\infty, |x|<+\infty \end{aligned} \tag{6}$$

We define the following dimensionless quantities

$$\begin{cases} \left(\overline{x},\overline{y},\overline{h}\right)=(x,y,h)\Big/c, \overline{T}_j=T_j\Big/\left(-Q_0c\Big/k_y^{(2)}\right), & j=1-3\\ \overline{\sigma}_{jkl}=\sigma_{jkl}\Big/\left(-E_0Q_0\alpha_2c\Big/k_y^{(2)}\right), & (k,l=x,y)\\ \left(\overline{u}_j,\overline{v}_j\right)=\left(u_j,v_j\right)\Big/\left(-Q_0\alpha_2c^2\Big/k_y^{(2)}\right) \end{cases} \tag{7}$$

$$\begin{cases} \left(\overline{\alpha}_{ij}^{(1)},\overline{\alpha}_{ij}^{(2)},\overline{\alpha}_{ij}^{(3)}\right)=\frac{\left(\alpha_{ij}^{(1)},\alpha_{ij}^{(2)},\alpha_{ij}^{(3)}\right)}{\alpha_0}, & (i,j=x,y)\\ \left(\overline{E}_{xx}^0,\overline{E}_{yy}^0\right)=\frac{\left(E_{xx}^0,E_{yy}^0\right)}{E_0} & \\ \left(\overline{C}_{ij}^{(1)},\overline{G}_{66}^{(1)},\overline{C}_{ij}^{(2)},\overline{G}_{66}^{(2)},\overline{C}_{ij}^{(3)},\overline{G}_{66}^{(3)}\right)=\frac{\left(C_{ij}^{(1)},G_{66}^{(1)},C_{ij}^{(2)},G_{66}^{(2)},C_{ij}^{(3)},G_{66}^{(3)}\right)}{E_0}, & (i,j=1,2) \end{cases} \tag{8}$$

where α_0 and E_0 are the typical values of the coefficient of linear thermal expansion and the Young's modulus of elasticity for the homogeneous orthotropic substrate, respectively. But for simplicity, in what follows, the bar appearing with the dimensionless quantities is omitted.

The Duhamel–Neumann constitutive equations for the plane thermo-elastic problem are given by Nowinski (1978)

$$\sigma_{xx} = C_{11}\frac{\partial u}{\partial x}+C_{12}\frac{\partial v}{\partial y}-\theta_1 T, \quad \sigma_{yy} = C_{12}\frac{\partial u}{\partial x}+C_{22}\frac{\partial v}{\partial y}-\theta_2 T, \quad \sigma_{xy} = C_{66}\left(\frac{\partial u}{\partial y}+\frac{\partial v}{\partial x}\right) \tag{9}$$

in which

$$\theta_1 = C_{11}\alpha_{xx} + C_{12}\alpha_{yy}, \quad \theta_2 = C_{12}\alpha_{xx} + C_{22}\alpha_{yy}, \quad C_{66} = G_{xy} \tag{10}$$

The elastic stiffness coefficients and the coefficients of the linear thermal expansion in dimensionless form are modeled to take the following forms

$$\begin{cases} \left(C_{11}^{(1)}, C_{12}^{(1)}, C_{22}^{(1)}, C_{66}^{(1)}\right) = \left(C_{11}^{(2)}, C_{12}^{(2)}, C_{22}^{(2)}, C_{66}^{(2)}\right)\exp(\beta y) \\ \left(\alpha_{xx}^{(1)}, \alpha_{yy}^{(1)}\right) = \left(\alpha_{xx}^{(2)}, \alpha_{yy}^{(2)}\right)\exp(\gamma y) \end{cases} \tag{11}$$

where superscripts 1, 2 refer to the FGOS and the homogeneous orthotropic substrate *II*, respectively, β and γ are graded parameters. The properties of material 3 can be found in Eq. (11) when y is taken as h. In Eq. (11), elastic stiffness coefficients in dimensionless form can be represented by the Young's moduli and the Poisson's ratios as

$$C_{11}^{(2)} = \frac{E_{xx}^{(2)}}{1-\nu_{yx}\nu_{xy}}, \quad C_{22}^{(2)} = \frac{E_{yy}^{(2)}}{1-\nu_{yx}\nu_{xy}}, \quad C_{12}^{(2)} = \frac{E_{yy}^{(2)}\nu_{xy}}{1-\nu_{yx}\nu_{xy}} \tag{12}$$

where ν_{ij} are the Poisson's ratios and assumed to be constant. $E_{xx}^{(2)}$ and $E_{yy}^{(2)}$ are Young's moduli for the homogeneous orthotropic substrate *II*, respectively.

Substituting Eq. (9) into the equations of equilibrium for the forces reduces these equations to the forms

$$\begin{cases} C_{11}^{(2)}\frac{\partial^2 u_1}{\partial x^2} + C_{66}^{(2)}\frac{\partial^2 u_1}{\partial y^2} + \left(C_{12}^{(2)} + C_{66}^{(2)}\right)\frac{\partial^2 v_1}{\partial x\partial y} + \beta C_{66}^{(2)}\left(\frac{\partial u_1}{\partial y} + \frac{\partial v_1}{\partial x}\right) = \theta_1^{(2)} e^{\gamma y}\frac{\partial T_1}{\partial x} \\ C_{22}^{(2)}\frac{\partial^2 v_1}{\partial y^2} + C_{66}^{(2)}\frac{\partial^2 v_1}{\partial x^2} + \left(C_{12}^{(2)} + C_{66}^{(2)}\right)\frac{\partial^2 u_1}{\partial x\partial y} + \beta\left(C_{12}^{(2)}\frac{\partial u_1}{\partial x} + C_{22}^{(2)}\frac{\partial v_1}{\partial y}\right) = \theta_2^{(2)} e^{\gamma y}\left[(\beta+\gamma)T_1 + \frac{\partial T_1}{\partial y}\right] \end{cases} \tag{13}$$

$$\begin{cases} C_{11}^{(2)}\dfrac{\partial^2 u_2}{\partial x^2} + C_{66}^{(2)}\dfrac{\partial^2 u_2}{\partial y^2} + \left(C_{12}^{(2)} + C_{66}^{(2)}\right)\dfrac{\partial^2 v_2}{\partial x\partial y} = \theta_1^{(2)}\dfrac{\partial T_2}{\partial x} \\ C_{22}^{(2)}\dfrac{\partial^2 v_2}{\partial y^2} + C_{66}^{(2)}\dfrac{\partial^2 v_2}{\partial x^2} + \left(C_{12}^{(2)} + C_{66}^{(2)}\right)\dfrac{\partial^2 u_2}{\partial x\partial y} = \theta_2^{(2)}\dfrac{\partial T_2}{\partial y} \end{cases} \tag{14}$$

$$\begin{cases} C_{11}^{(2)}\dfrac{\partial^2 u_3}{\partial x^2}+C_{66}^{(2)}\dfrac{\partial^2 u_3}{\partial y^2}+\left(C_{12}^{(2)}+C_{66}^{(2)}\right)\dfrac{\partial^2 v_3}{\partial x\partial y}=\theta_1^{(2)}e^{\gamma h}\dfrac{\partial T_3}{\partial x} \\ C_{22}^{(2)}\dfrac{\partial^2 v_3}{\partial y^2}+C_{66}^{(2)}\dfrac{\partial^2 v_3}{\partial x^2}+\left(C_{12}^{(2)}+C_{66}^{(2)}\right)\dfrac{\partial^2 u_3}{\partial x\partial y}=\theta_2^{(2)}e^{\gamma h}\dfrac{\partial T_3}{\partial y} \end{cases} \tag{15}$$

Boundary conditions

The temperature filed can be provided using the following boundary condition

$$T_1(x,y)=T_3(x,y) \quad |x|<+\infty,\ y=h \tag{16}$$

$$\frac{\partial T_1(x,y)}{\partial y}=\begin{cases} -Bi\big(T_1(x,y)-T_2(x,y)\big) & |x|\le c, \quad y=0 \\ \frac{\partial T_2(x,y)}{\partial y} & |x|<+\infty,\ y=0 \\ \frac{\partial T_3(x,y)}{\partial y} & |x|<+\infty,\ y=h \\ -Q_0/k_y^{(3)} & y\to+\infty, \quad |x|<+\infty \end{cases} \tag{17}$$

where $Bi=1/k_y^{(1)}(0)/R_c$ is dimensionless thermal resistance through the crack region. R_c is the thermal resistance through the crack region.

The boundary conditions of the stress and displacement field can be given by

$$\sigma_{1xy}(x,y)=\begin{cases} 0 & y=0, \quad |x|\le c \\ \sigma_{3xy}(x,y) & y=h \end{cases}, \quad \sigma_{1yy}(x,y)=\begin{cases} 0 & y=0, \quad |x|\le c \\ \sigma_{3xy}(x,y) & y=h \end{cases}, \tag{18}$$

$$u_1(x,h^-)=u_3(x,h^+) \quad v_1(x,h^-)=v_3(x,h^+) \quad |x|<\infty \tag{19}$$

Heat conduction problem

By using Fourier transform, the solutions of Eqs. (4) and (5) are given by

$$\begin{cases} T_1(x,y)=\int_{-\infty}^{+\infty}\left(M_1(\omega)\exp(s_1y)+M_2(\omega)\exp(s_2y)\right)\exp(-i\omega x)d\omega+\frac{1-e^{-\delta y}}{\delta}, & 0<y<h \\ T_2(x,y)=\int_{-\infty}^{+\infty}\left(M_3(\omega)\exp(p_1y)+M_4(\omega)\exp(p_2y)\right)\exp(-i\omega x)d\omega+y, & y\le 0 \\ T_3(x,y)=\int_{-\infty}^{+\infty}\left(M_5(\omega)\exp(o_1y)+M_6(\omega)\exp(o_2y)\right)\exp(-i\omega x)d\omega+e^{-\delta h}y+1/\delta-\frac{1+\delta h}{\delta}e^{-\delta h}, & y\ge h \end{cases} \tag{20}$$

where $M_k(\omega)(k=1-6)$ can be found in "Appendix 1". s_k, p_k and o_k are the roots of the characteristic polynomials, which can be given by

$$s_{1,2}=\frac{1}{2}\left(-\delta\pm\sqrt{\delta^2+4k_{xy0}\omega^2}\right), \quad p_{1,2}=\pm\sqrt{k_{xy0}}|\omega|, \quad o_{1,2}=\pm\sqrt{k_{xy0}}|\omega| \tag{21}$$

Introducing the unknown density function

$$\phi(x)=\frac{\partial}{\partial x}\left[T_1(x,0^+)-T_2(x,0^-)\right] \tag{22}$$

From (17), we obtain

$$\int_{-1}^{+1}\left(\frac{1}{u-x}+H(x,u)\right)\phi(u)du=\frac{-2\pi}{\sqrt{k_{xy0}}} \tag{23}$$

where the kernel $H(x,u)$ can be found in "Appendix 1".

Thermal stress analysis

By using the standard Fourier transforms to Eqs. (13)–(15), following results for the displacement fields for the FGOS and two homogeneous orthotropic media are obtained

$$\begin{cases} u_1(x,y) = \int_{-\infty}^{+\infty} \left(\sum_{j=1}^{4} C_j(\omega) e^{m_j y} \right) e^{-ix\omega} d\omega + \int_{-\infty}^{+\infty} \left(\sum_{j=1}^{2} \frac{\xi_j(\omega)}{d_j(\omega)} e^{(\gamma+s_j)y} \right) e^{-ix\omega} d\omega \\ v_1(x,y) = \int_{-\infty}^{+\infty} \left(\sum_{j=1}^{4} C_j(\omega) q_j(\omega) e^{m_j y} \right) e^{-ix\omega} d\omega + \int_{-\infty}^{+\infty} \left(\sum_{j=1}^{2} \frac{\xi_{j+2}(\omega)}{d_j(\omega)} e^{(\gamma+s_j)y} \right) e^{-ix\omega} d\omega + \chi_1 e^{\gamma y} + \chi_2 e^{(\gamma-\delta)y} \end{cases} \tag{24}$$

$$\begin{cases} u_2(x,y) = \int_{-\infty}^{+\infty} \left(C_5(\omega) e^{n_1 y} + C_6(\omega) e^{n_2 y} + \frac{\xi_5(\omega)}{d_3(\omega)} e^{(\gamma+p_1)y} \right) e^{-i\omega x} d\omega \\ v_2(x,y) = \int_{-\infty}^{+\infty} \left(C_5(\omega) q_5(\omega) e^{n_1 y} + C_6(\omega) q_6(\omega) e^{n_2 y} + \frac{\xi_6(\omega)}{d_3(\omega)} e^{(\gamma+p_1)y} \right) e^{-i\omega x} d\omega + \frac{\theta_2^{(2)}}{2C_{12}^{(2)}} y^2 \end{cases} \tag{25}$$

$$\begin{cases} u_3(x,y) = \int_{-\infty}^{+\infty} \left(C_7(\omega) e^{n_3 y} + C_8(\omega) e^{n_4 y} + \frac{\xi_7(\omega)}{d_4(\omega)} e^{(\gamma+o_2)y} \right) e^{-i\omega x} d\omega \\ v_3(x,y) = \int_{-\infty}^{+\infty} \left(C_7(\omega) q_7(\omega) e^{n_3 y} + C_8(\omega) q_8(\omega) e^{n_4 y} + \frac{\xi_8(\omega)}{d_4(\omega)} e^{(\gamma+o_2)y} \right) e^{-i\omega x} d\omega + \chi_1 e^{\gamma h} + \chi_2 e^{(\gamma-\delta)h} \end{cases} \tag{26}$$

where $C_j(\omega)(j = 1-8)$ are unknown function. $\xi_j, q_j(j = 1-8)$, $d_j(j = 1-4)$, $\chi_j(j = 1,2)$ are given in "Appendix 1". $m_j(j = 1-4)$ and $n_j(j = 1-4)$ are the roots of the characteristic polynomials, which can be given by

$$m_{1,2} = \frac{1}{2}\left(-\beta - \sqrt{\beta^2 - 2\Delta_1 \pm 2\sqrt{(\Delta_1)^2 - 4\Delta_2}} \right) \tag{27}$$

$$m_{3,4} = \frac{1}{2}\left(-\beta + \sqrt{\beta^2 - 2\Delta_1 \pm 2\sqrt{(\Delta_1)^2 - 4\Delta_2}} \right) \tag{28}$$

$$n_{1,2} = -\frac{1}{2}\sqrt{-2\Delta_3 \pm 2\sqrt{(\Delta_3)^2 - 4\Delta_4}}, \quad n_{3,4} = \frac{1}{2}\sqrt{-2\Delta_3 \pm 2\sqrt{(\Delta_3)^2 - 4\Delta_4}} \tag{29}$$

where

$$\Delta_1 = \omega^2 \left(\frac{(C_{12}^{(2)})^2}{C_{22}^{(2)} C_{66}^{(2)}} - \frac{C_{11}^{(2)}}{C_{66}^{(2)}} + 2\frac{C_{12}^{(2)}}{C_{22}^{(2)}} \right),$$

$$\Delta_2 = \omega^4 \frac{C_{11}^{(2)}}{C_{22}^{(2)}} + \omega^2 \beta^2 \frac{C_{12}^{(2)}}{C_{22}^{(2)}}, \quad \Delta_3 = \Delta_1, \quad \Delta_4 = \omega^4 \frac{C_{11}^2}{C_{22}^2}$$

Solution procedure and near-tip field intensity factors

Introducing the density functions

$$\Phi_1(x) = \frac{\partial}{\partial x}\left[u(x,0^+) - u(x,0^-) \right], \quad \Phi_2(x) = \frac{\partial}{\partial x}\left[v(x,0^+) - v(x,0^-) \right] \tag{30}$$

Substituting Eqs. (24)–(26) into Eqs. (18)–(19), we obtain

$$\begin{cases} \int_{-1}^{1} \left\{ \left[\dfrac{1}{u-x} + K_{11}(x,u) \right] \Phi_1(u) + K_{12}(x,u)\Phi_2(u) \right\} du = \dfrac{2\pi \cdot \omega_1^T(x)}{\sqrt{k_{xy0}}} \\ \int_{-1}^{1} \left\{ K_{21}(x,u)\Phi_1(u) + \left[\dfrac{1}{u-x} + K_{22}(x,u) \right] \Phi_2(u) \right\} du = \dfrac{2\pi \cdot \omega_2^T(x)}{\sqrt{k_{xy0}}} \end{cases} \tag{31}$$

where $K_{ij}(x,u)(i,j=1,2)$, $\omega_1(x)^T, \omega_2(x)^T$ are given in "Appendix 2".

The singular integral Eq. (31) are solved numerically with the unknown density functions $R_1(u)$ and $R_2(u)$ having the following form

$$\begin{cases} \Phi_1(u) = \frac{R_1(u)}{\sqrt{1-u^2}} & R_1(u) = \sum_{n=1}^{N} b_n T_n(u) \\ \Phi_2(u) = \frac{R_2(u)}{\sqrt{1-u^2}} & R_2(u) = \sum_{n=1}^{N} c_n T_n(u) \end{cases} \tag{32}$$

Once $R_1(u)$ and $R_2(u)$ have been determined, the thermal stress intensity factors ahead of the crack tip can be defined and calculated as follows

$$\begin{cases} K_I(1) = \lim\limits_{x\to 1^+} \sqrt{2(x-1)}\sigma_{yy}(x,0) = -\frac{\sqrt{k_{xy0}}}{2} R_2(1), \\ K_I(-1) = \lim\limits_{x\to -1^-} \sqrt{2(-x-1)}\sigma_{yy}(x,0) = \frac{\sqrt{k_{xy0}}}{2} R_2(-1), \\ K_{II}(1) = \lim\limits_{x\to 1^+} \sqrt{2(x-1)}\sigma_{xy}(x,0) = -\frac{\sqrt{k_{xy0}}}{2} R_1(1), \\ K_{II}(-1) = \lim\limits_{x\to -1^-} \sqrt{2(-x-1)}\sigma_{xy}(x,0) = \frac{\sqrt{k_{xy0}}}{2} R_1(-1). \end{cases} \tag{33}$$

Numerical results and discussion

In this paper, the orthotropy and non-homogeneity parameters of Tyrannohex can be found in Ootao and Tanigawa (2005). The material properties can be given by

$$E_{xx} = 135\,\text{GPa}, \quad E_{yy} = 87\,\text{GPa}, \quad \nu_{xy} = 0.15, \quad \nu_{yx} = 0.09667, \quad \alpha_{xx} = 0.32 \times 10^{-5}/^{\circ}\text{C},$$
$$\alpha_{yy} = 0.32 \times 10^{-5}/^{\circ}\text{C}, \quad k_x = 2.81\ \text{W/m}\ ^{\circ}\text{C}, \quad k_y = 3.08\ \text{W/m}\ ^{\circ}\text{C}$$

In the presented results the values of the thermal stress intensity factors are normalized by $k_0 = E_2 Q_0 \alpha_2 \sqrt{c}/k_y^{(2)}$. The crack is located along the interval $-1 \le x \le 1$.

Figure 2a, b show the effects of the thermal conductivity parameter δ on the crack surface temperature when $Bi = 0.1$ and $Bi = 0.5$, respectively. From Fig. 2a, b, it can be found that the temperature jump across the crack surfaces increases with an decrease of the absolute values of δ. At the other hand, for smaller value of Bi, the temperature will become more pronounced. As expected, the temperature jump across the crack becomes more pronounced as the crack surfaces become more insulated, that is, as Bi decreases.

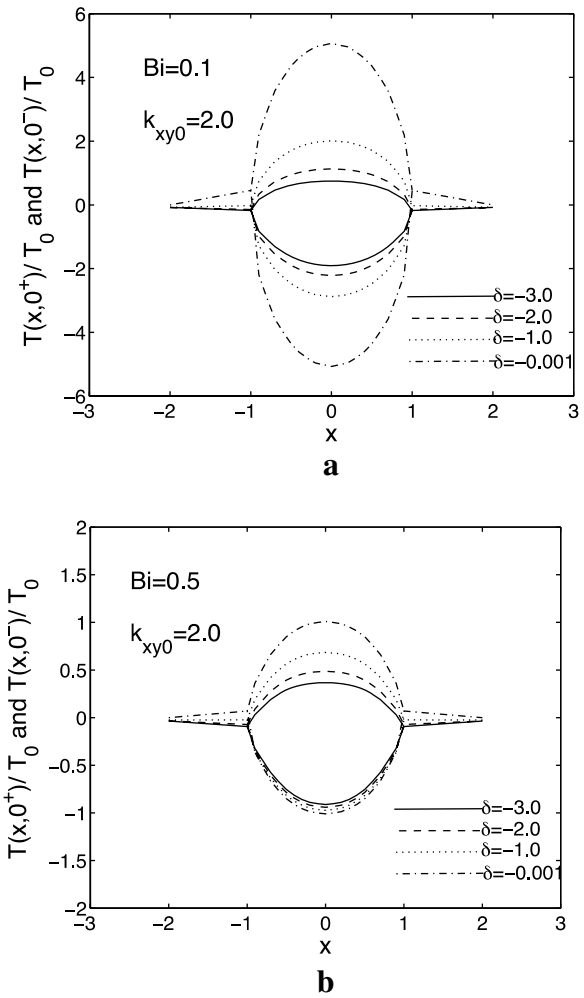

Fig. 2 Influences of thermal conductivity parameter δ on the normalized crack surfaces and crack extend line $y = 0$ temperatures $T(x, 0^+)/T_0$ and $T(x, 0^-)/T_0$,$T_0 = Q_0c/k_y^{(2)}$, $h = 1.0$, $k_{xy0} = 2.0$, **a** Bi = 0.1, **b** Bi = 0.5

Figure 3a, b show the effects of the thermal conductivity parameter δ and k_{xy0} on the mode I and $k_{xy0} = 0.5II$ thermal stress intensity factors. It can be found that the mode I thermal stress intensity factors increases with an increase of the thermal conductivity parameter δ for either or $k_{xy0} = 2.0$; while increases with an increase of k_{xy0} for both $\delta = -1.0$ and $\delta = 1.0$. And the values of mode II thermal stress intensity factors decreases with the increasing of the thermal conductivity parameter δ regardless of the value of k_{xy0}. Meanwhile, the values of mode II thermal stress intensity factors decreases with the increasing of an increase of k_{xy0} regardless of the value o $\alpha_{xx}^{(2)}$ f δ.

Figure 4a, b illustrate the effects of the stiffness parameter β and $E_{xx}^{(2)}$ on the mode I and II thermal stress intensity factors. It can be seen that the mode I thermal stress intensity factors increases with a decrease of the stiffness parameter β for both $E_{xx}^{(2)} = 0.5$ and

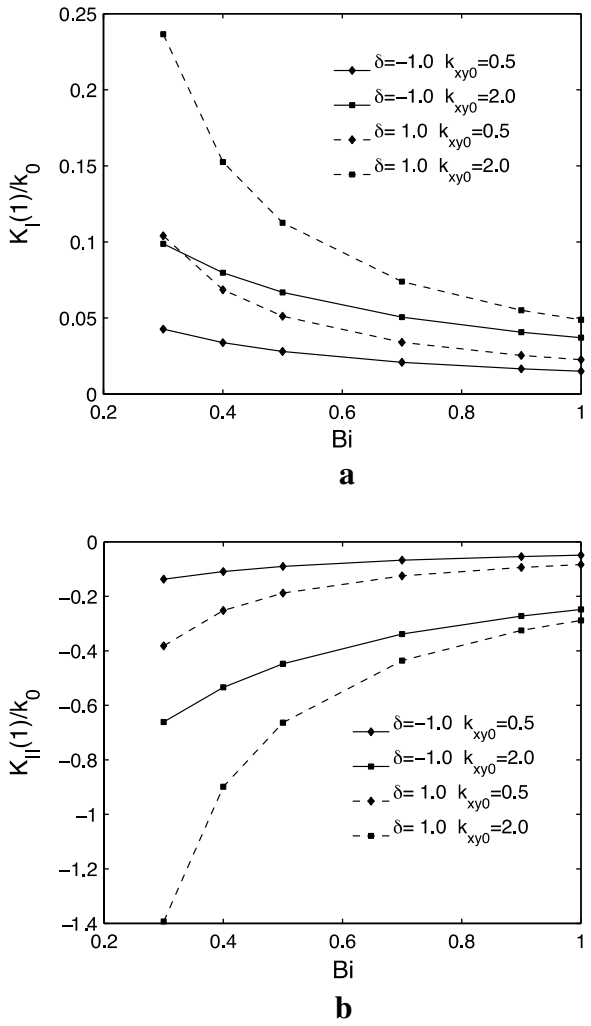

Fig. 3 Influences of the thermal conductivity parameter δ and k_{xy0} on the normalized thermal stress intensity factors, $h = 1.0$. **a** mode *I*. **b** mode *II*

$E_{xx}^{(2)} = 2.0$; while increases with an increase of $E_{xx}^{(2)}$ regardless of the value of the stiffness parameter β. For the mode *II* thermal stress intensity factors, the contrary is the case.

Figure 5a, b show the *II* effects of the thermal expansion parameter γ and on the mode *I* and *II* thermal stress intensity factors. It may be obtained that the absolute values of both mode *I* and mode *II* thermal stress intensity factors increases with an increase of the thermal expansion parameter γ for either $k_{xy0} = 0.5$ or $k_{xy0} = 2.0$; and the absolute values of both mode *I* and mode *II* thermal stress intensity factors increases with an increase of $\alpha_{xx}^{(2)}$.

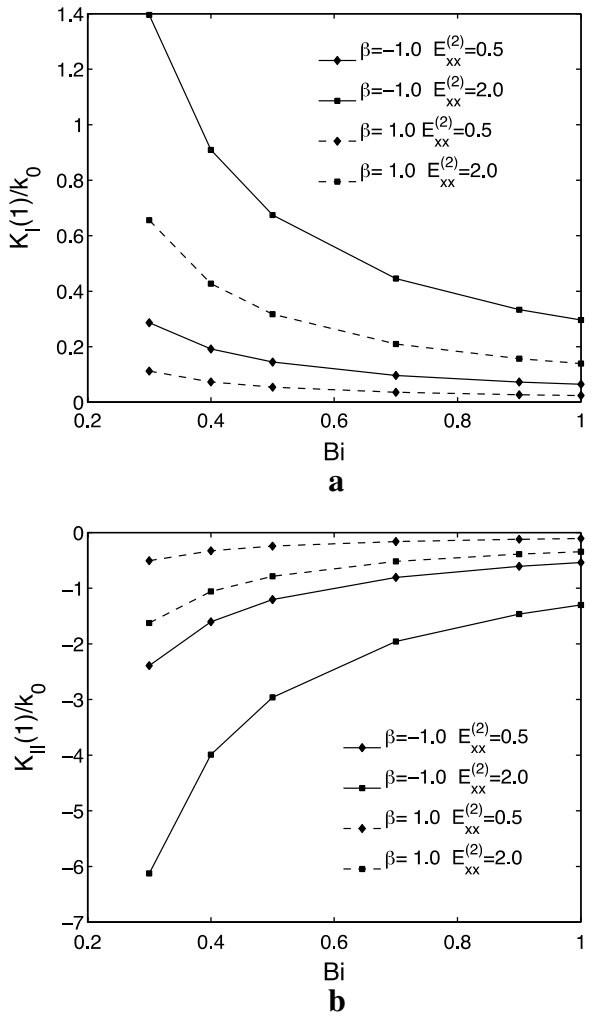

Fig. 4 Influences of the stiffness parameter β and $E_{xx}^{(2)}$ on the normalized mode thermal stress intensity factors. **a** *I*. **b** mode *II*

Figure 6a, b illustrate the effects of different thickness of functionally graded orthotropic strip on the mode I and II thermal stress intensity factors when $\delta = -1.0$ and $\delta = 1.0$, respectively. We can see that the mode I and thermal stress intensity factors increase or decrease with the increasing of h, and then reach a steady value.

Conclusions

In this paper, thermo-mechanical stress and displacement fields for an interface crack between an orthotropic functionally graded interlayer and two homogeneous orthotropic media are obtained. In addition to the mechanical fields, temperature fields are

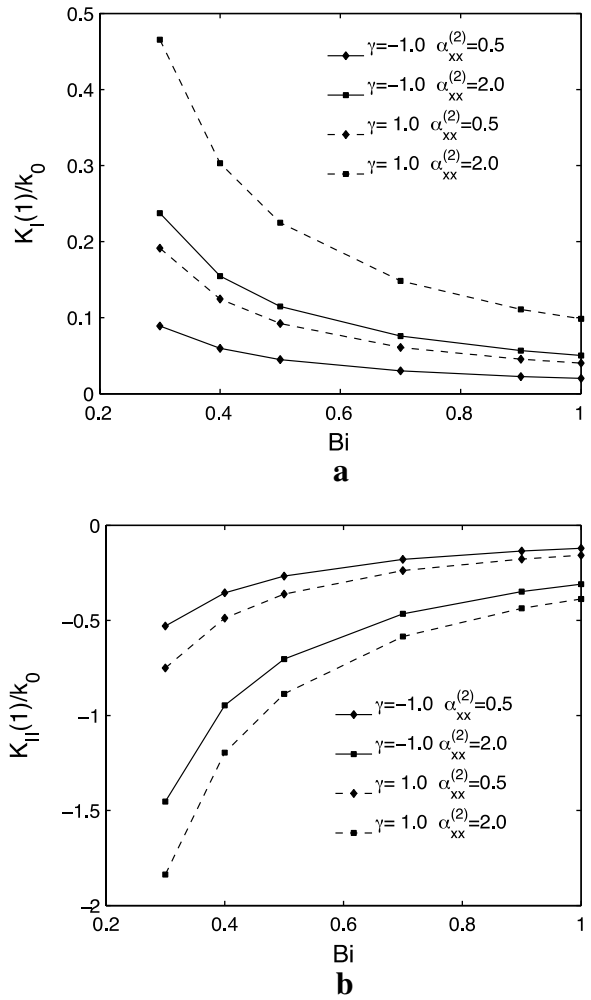

Fig. 5 Influences of the thermal expansion parameter γ and $\alpha_{xx}^{(2)}$ on the normalized mode thermal stress intensity factors. **a** *I*. **b** *II*

also developed for exponentially varying thermal properties along the gradation direction. TSIFS are numerically calculated based on a singular integral equation derived from the dislocation density along the crack faces. The variations in temperature distribution and the thermal stress intensity factors due to the change in non-homogeneity parameters of the material thermo-elastic properties, the orthotropy parameters and the dimensionless thermal resistance are investigated.

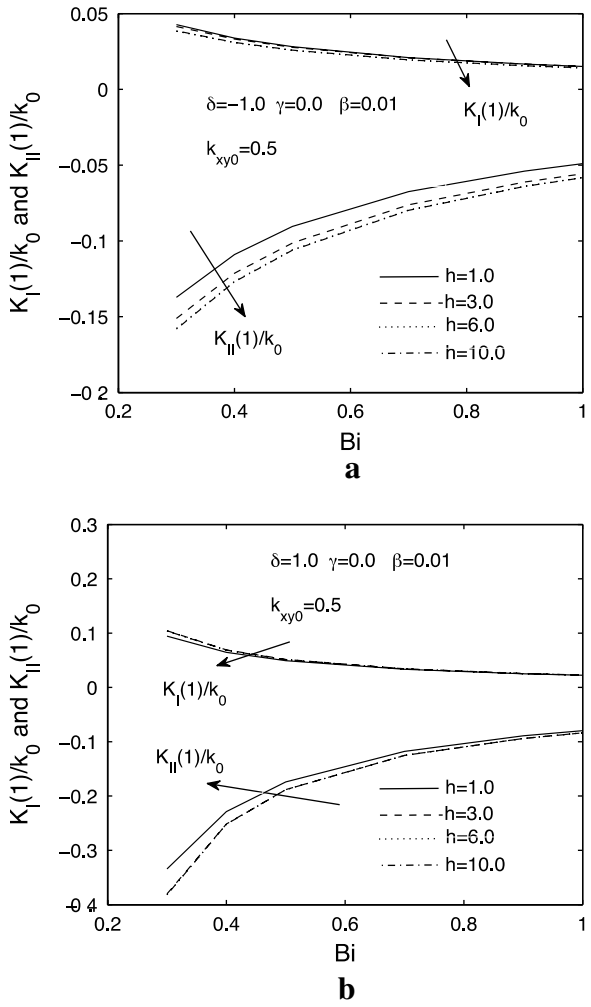

Fig. 6 Influences of the thickness *h* of the functionally graded orthotropic strip on the normalized mode *I* and mode *II* thermal stress intensity factors, **a** $\delta = -1.0$, **b** $\delta = 1.0$

Authors' contributions

SHD established the model and completed the derivation and calculation. XL analyzed the numerical results. Both authors read and approved the final manuscript.

Acknowledgements

Financial support from the National Natural Science Foundation of China (11261045, 11261041, 11472193), the China Scholarship Council (CSC), the Fundamental Research Funds for the Central Universities (1330219162) and Shanghai Pujiang Program (14PJ1409100) are gratefully acknowledged.

Competing interests

The authors declare that they have no competing interests.

Appendix 1

The expressions of $M_j(w)(j = 1-6)$ are given by

$$\begin{cases} M_1(\omega) = \frac{ip_1(o_2-s_2)e^{s_2h}}{2\pi\omega((s_1-o_2)(p_1-s_2)e^{s_1h}+(o_2-s_2)(p_1-s_1)e^{s_2h})}\int_{-1}^{1}\phi(x)e^{i\omega x}dx \\ M_2(\omega) = \frac{ip_1(s_1-o_2)e^{s_1h}}{2\pi\omega((s_1-o_2)(p_1-s_2)e^{s_1h}+(o_2-s_2)(p_1-s_1)e^{s_2h})}\int_{-1}^{1}\phi(x)e^{i\omega x}dx \\ M_3(\omega) = \frac{i[s_1(o_2-s_2)e^{s_2h}+s_2(s_1-o_2)e^{s_1h}]}{2\pi\omega((s_1-o_2)(p_1-s_2)e^{s_1h}+(o_2-s_2)(p_1-s_1)e^{s_2h})}\int_{-1}^{1}\phi(x)e^{i\omega x}dx \\ M_4(\omega) = M_5(\omega) = 0 \\ M_6(\omega) = \frac{ip_1(s_1-s_2)e^{(s_1+s_2-o_2)h}}{2\pi\omega((s_1-o_2)(p_1-s_2)e^{s_1h}+(o_2-s_2)(p_1-s_1)e^{s_2h})}\int_{-1}^{1}\phi(x)e^{i\omega x}dx \end{cases} \tag{34}$$

The kernel function $H(x,u)$ is

$$H(x,u) = \int_0^{+\infty}\frac{-2}{\sqrt{k_{xy0}}\omega}\left[\frac{s_1p_1(o_2-s_2)e^{s_2h}+s_2p_1(s_1-o_2)e^{s_1h}}{(s_1-o_2)(p_1-s_2)e^{s_1h}+(o_2-s_2)(p_1-s_1)e^{s_2h}}+Bi-1\right]\sin[\omega(u-x)]d\omega \tag{35}$$

The expressions of $\xi_j, q_j(j = 1-8), d_j(j = 1-4), \chi_j(j = 1,2)$ are given by

$$\begin{aligned}\xi_j = {} & i\omega M_j\left[(\gamma+s_j)(\gamma+s_j+\beta)\left(\theta_2^2C_{12}^2-\theta_1^2C_{22}^2\right)\right] \\ & + C_{66}^2\left[\omega^2\theta_1^2+(\gamma+s_j+\beta)^2\theta_2^2\right], \quad j = 1,2\end{aligned} \tag{36}$$

$$\begin{aligned}\xi_j = {} & \omega^2M_{j-2}\left\{\left[(\gamma+s_{j-2}+\beta)\left(\theta_1^2C_{12}^2-\theta_2^2C_{11}^2\right)\right]\right. \\ & \left.+(\gamma+s_{j-2})C_{66}^2\left[\omega^2\theta_1^2+(\gamma+s_{j-2}+\beta)^2\theta_2^2\right]\right\} \quad j = 3,4\end{aligned} \tag{37}$$

$$\xi_5 = i\omega M_3\left[p_1^2\left(\theta_2^2C_{12}^2-\theta_1^2C_{22}^2\right)\right]+C_{66}^2\left[\omega^2\theta_1^2+p_1^2\theta_2^2\right] \tag{38}$$

$$\xi_6 = \omega^2M_3\left[p_1\left(\theta_1^2C_{12}^2-\theta_2^2C_{22}^2\right)\right]+p_1C_{66}^2\left[\omega^2\theta_1^2+p_1^2\theta_2^2\right] \tag{39}$$

$$\xi_7 = i\omega M_6\left[o_2^2\left(\theta_2^2C_{12}^2-\theta_1^2C_{22}^2\right)\right]+C_{66}^2\left[\omega^2\theta_1^2+o_2^2\theta_2^2\right] \tag{40}$$

$$\xi_8 = \omega^2M_6\left[o_2\left(\theta_1^2C_{12}^2-\theta_2^2C_{11}^2\right)\right]+o_2C_{66}^2\left[\omega^2\theta_1^2+o_2^2\theta_2^2\right] \tag{41}$$

$$q_j(\omega) = \frac{i\omega\left[m_j\left(C_{12}^2+C_{66}^2\right)+\beta C_{12}^2\right]}{m_j(m_j+\beta)C_{22}^2-\omega^2C_{66}^2}, \quad j = 1-4 \tag{42}$$

$$q_j(\omega) = \frac{i\omega n_{j-4}\left(C_{12}^2+C_{66}^2\right)}{n_{j-4}^2C_{22}^2-\omega^2C_{66}^2}, \quad j = 5-8 \tag{43}$$

$$\begin{aligned}d_j(\omega) = {} & C_{66}^2C_{12}^2[C_{11}^2\omega^4+\omega^2[(\gamma+s_j)^2+(\gamma+s_j+\beta)^2]+(\gamma+s_j)^2 \\ & (\gamma+s_j+\beta)^2C_{22}^2]+\omega^2(\gamma+s_j)(\gamma+s_j+\beta)[(C_{12}^2)^2-C_{11}^2C_{22}^2], \quad j = 1-2\end{aligned} \tag{44}$$

$$d_3(\omega) = C_{66}^2\left[C_{11}^2\omega^2+2\omega^2p_1^2C_{12}^2+p_1^4C_{22}^2\right]+\omega^2p_1^2\left[\left(C_{12}^2\right)^2-C_{11}^2C_{22}^2\right] \tag{45}$$

$$d_4(\omega) = C_{66}^2\left[C_{11}^2\omega^2 + 2\omega^2 o_2^2 C_{12}^2 + o_2^4 C_{22}^2\right] + \omega^2 o_2^2\left[\left(C_{12}^2\right)^2 - C_{11}^2 C_{22}^2\right] \tag{46}$$

$$\chi_1 = \frac{\theta_2^2}{\delta C_{22}^2 \gamma} \quad \chi_2 = -\frac{\theta_2^2}{\delta C_{22}^2(\gamma - \delta)} \tag{47}$$

Appendix 2

The expressions of $K_{ij}(x,u)(i,j=1,2)$,$\omega_1(x)^T, \omega_2(x)^T$ are given by

$$K_{11}(x,u) = \lim_{y\to 0^-}\int_0^{+\infty}\left(\frac{2}{\omega\sqrt{k_{xy0}}}\left(\frac{A_{22}D_{16}}{D}e^{n_2 y} - \frac{A_{21}D_{15}}{D}e^{n_1 y}\right) - 1\right)\sin[\omega(u-x)]d\omega \tag{48}$$

$$K_{12}(x,u) = \lim_{y\to 0^-}\int_0^{+\infty}\frac{2i}{\omega\sqrt{k_{xy0}}}\left(\frac{A_{22}D_{26}}{D}e^{n_2 y} - \frac{A_{21}D_{25}}{D}e^{n_1 y}\right)\cos[\omega(u-x)]d\omega \tag{49}$$

$$K_{21}(x,u) = \lim_{y\to 0^-}\int_0^{+\infty}\frac{2i}{\omega\sqrt{k_{xy0}}}\left(\frac{A_{24}D_{16}}{D}e^{n_2 y} - \frac{A_{23}D_{15}}{D}e^{n_1 y}\right)\cos[\omega(u-x)]d\omega \tag{50}$$

$$K_{22}(x,u) = \lim_{y\to 0^-}\int_0^{+\infty}\left(\frac{2}{\omega\sqrt{k_{xy0}}}\left(\frac{A_{24}D_{16}}{D}e^{n_2 y} - \frac{A_{23}D_{15}}{D}e^{n_1 y}\right) - 1\right)\sin[\omega(u-x)]d\omega \tag{51}$$

$$\begin{cases}\omega_1^T(x) = \int_{-\infty}^{+\infty}\left(\sum_{j=1}^{8} I_j J_{1j} - B_{23}e^{-i\omega x}\right)dx \\ \omega_2^T(x) = \int_{-\infty}^{+\infty}\left(\sum_{j=1}^{8} I_j J_{2j} - B_{21} - B_{22}\right)e^{-i\omega x}dx\end{cases} \tag{52}$$

with

$$I_1 = \xi_5/d_3 - \sum_{j=1}^{2}\xi_j/d_j \quad I_2 = \xi_6/d_3 - \sum_{j=1}^{2}\xi_{j+2}/d_j \tag{53}$$

$$I_3 = e^{(\gamma+o_2)h}q_7/d_4 - \sum_{j=1}^{2}e^{(\gamma+s_j)h}\xi_j/d_j \quad I_4 = e^{(\gamma+o_2)h}q_8/d_4 - \sum_{j=1}^{2}e^{(\gamma+s_j)h}\xi_{j+2}/d_j \tag{54}$$

$$I_5 = B_{23} - \sum_{j=1}^{2}F_{1j} \quad I_6 = B_{21} + B_{22} - \sum_{j=1}^{2}B_{1j} \tag{55}$$

$$I_7 = e^{(\gamma+o_2)h}B_{31} + e^{o_2 h}B_{32} - \sum_{j=1}^{2}e^{(\gamma+s_j)h}B_{1j} \quad I_8 = e^{(\gamma+o_2)h}B_{33} - \sum_{j=1}^{2}e^{(\gamma+s_j)h}F_{1j} \tag{56}$$

$$J_{1j} = (-1)^{j+1}\left(\frac{A_{22}D_{j6}}{D} - \frac{A_{21}D_{j5}}{D}\right) \quad J_{2j} = (-1)^{j+1}\left(\frac{A_{24}D_{j6}}{D} - \frac{A_{23}D_{j5}}{D}\right) \tag{57}$$

$$A_{1j} = (-i\omega)C_{12}^2 + C_{22}^2 m_j q_j \quad j = 1-4 \tag{58}$$

$$B_{1j} = \left[(-i\omega)C_{12}^2\xi_j + C_{22}^2(\gamma + s_j)\xi_{j+2}\right]/d_j - \theta_2^{(2)}M_j \quad E_{1j} = C_{66}^2(m_j - i\omega q_j) \tag{59}$$

$$F_{1j} = C_{66}^2\left[(\gamma + s_j)\xi_j - i\omega\xi_{j+2}\right]/d_j \quad j = 1-4 \tag{60}$$

$$A_{21} = C_{22}^2 n_1 q_5 - i\omega C_{12}^2 \quad A_{22} = C_{22}^2 n_2 q_6 - i\omega C_{12}^2 \tag{61}$$

$$B_{21} = \left[C_{22}^2(\gamma + p_1)\xi_6 - i\omega C_{12}^2\right]/d_3 \quad B_{22} = -\theta_2^2 M_3 \tag{62}$$

$$A_{23} = C_{66}^2(n_1 - i\omega q_5) \quad A_{24} = C_{66}^2(n_2 - i\omega q_6) \tag{63}$$

$$B_{23} = C_{66}^2[(\gamma + p_1)\xi_5 - i\omega\xi_6]/d_3 \quad A_{31} = C_{22}^2 n_3 q_7 - i\omega C_{12}^2 \tag{64}$$

$$A_{32} = C_{22}^2 n_4 q_8 - i\omega C_{12}^2 \quad B_{31} = \left[C_{22}^2(\gamma + o_2)\xi_8 - i\omega C_{12}^2\xi_7\right]/d_4 \tag{65}$$

$$B_{32} = -\theta_2^2 M_6 e^{\gamma h} \quad A_{33} = C_{66}^2(n_3 - i\omega q_7) \tag{66}$$

$$A_{34} = C_{66}^2(n_4 - i\omega q_8) \quad B_{33} = C_{66}^2[(\gamma + o_2)\xi_7 - i\omega\xi_8]/d_4 \tag{67}$$

Here D is the determinant of the $D_{ij}(i,j = 1-8)$. D_{ij} is the sub-determinant of the linear system of Eqs. (24)–(26) corresponding to the elimination of the *ith* row and *j*th column.

Received: 13 January 2016 Accepted: 18 August 2016
Published online: 06 September 2016

References

Chen J (2005) Determination of thermal stress intensity factors for interface crack in a graded orthotropic coating-substrate structure. Int J Fract 133:303–328

Cheng ZQ, Meguid SA, Zhong Z (2010) Thermo-mechanical behavior of a viscoelastic FGMs coating containing an interface crack. Int J Fract 164:15–29

Choi HJ (2003) Thermoelastic problem of steady-state heat flow disturbed by a crack perpendicular to the graded interfacial zone in bonded materials. J Therm Stress 26:997–1030

Choi HJ, Lee KY, Jin TE (1998) Collinear cracks in a layered half-plane with a graded nonhomogenous interfacial zone Part II: thermal shock response. Int J Fract 94:123–135

Dag S (2006) Thermal fracture analysis of orthotropic functionally graded materials using an equivalent domain integral approach. Eng Fract Mech 73:2802–2828

Dai KY, Liu GR, Han X, Lim KM (2005) Thermomechanical analysis of functionally graded material (FGM) plates using element-free Galerkin method. Comput Struct 83:1487–1502

Ding SH, Li X (2014) The collinear cracks problem for an orthotropic functionally graded coating-substrate structure. Arch Appl Mech 84:291–307

Ding SH, Li X (2015) Thermoelastic analysis of nonhomogeneous structural materials with an interface crack under uniform heat flow. Appl Math Comput 271:22–33

Ding SH, Zhou YT, Li X (2014) Interface crack problem in layered orthotropic materials under thermo-mechanical loading. Int J Solids Struct 25–26:4221–4229
Ding SH, Zhou YT, Li X (2015) Thermal stress analysis of an embedded crack in a graded orthotropic coating-substrate structure. J Therm Stress 9:1005–1021
El-Borgi S, Hidri L (2006) An embedded crack in a graded coating bonded to a homogeneous substrate under thermo-mechanical loading. J Therm Stress 29:439–466
Fujimoto T, Noda N (2001) Influence of the compositional profile of functionally graded material on the crack path under thermal shock. J Am Ceram Soc 84:1480–1486
Han JC, Wang BL (2006) Thermal shock resistance enhancement of functionally graded materials by multiple cracking. Acta Mater 54:963–973
Itou S (2004) Thermal stresses around a crack in the nonhomogeneous interfacial layer between two dissimilar elastic half-planes. Int J Solids Struct 41:923–945
Jin ZH, Noda N (1991) Transient thermal stress intensity factors for a crack in a semi-infinite plate of a functionally gradient material. Int J Solids Struct 31:203–218
Kim J, Paulino G (2002) Mixed-mode fracture of orthotropic functionally graded materials using finite elements and the modified crack closure method. Eng Fract Mech 69:1557–1586
Miyamoto Y, Kaysser WA, Rabin BH, Kawasaki A, Ford RG (eds) (1999) Functionally graded materials: design, processing, and applications. Kluwer, Berlin
Natarajana S, Baizb PM, Bordasa S, Rabczukc T, Kerfridena P (2011) Natural frequencies of cracked functionally graded material plates by the extended finite element method. Compos Struct 93:3082–3092
Niino M, Hirai T, Watanabe R (1987) The functionally gradient materials. Jpn Soc Compos Mater 13:257–264
Nowinski JL (1978) Theory of thermoelasticity with applications. Sijthoff & Noordhoff, Alphen aan den Rijn
Ootao Y, Tanigawa Y (2005) Transient thermal stresses of orthotropic functionally graded thick strip due to nonuniform heat supply. Struct Eng Mech 20:559–573
Pathak H, Singh A, Singh IV (2013) Fatigue crack growth simulations of bi-material interfacial cracks under thermo-elastic loading by extended finite element method. Eur J Comput Mech 22:79–104
Pathak H, Singh A, Singh IV (2014) Fatigue crack growth simulations of homogeneous and bi-material interfacial cracks using element free Galerkin method. Appl Math Model 38:3093–3123
Sofiyev AH, Avcar M (2010) The stability of cylindrical shells containing an fgm layer subjected to axial load on the pasternak foundation. Engineering 4:228–236
Sofiyev AH, Zerin Z, Deniz A, Avcar M, Ozyigit P (2012) The stability analysis of FGM-Metal-FGM layered cylindrical shells under a lateral pressure. In: 11th International congress on advances in civil engineering, pp 0124–0132
Suresh S, Mortensen A (1998) Fundamentals of functionally graded materials, processing and thermo-mechanical behavior of graded metals and metal-ceramic composites. IOM Communications Ltd, London
Wang BL, Mai YW, Zhang XH (2004) Thermal shock resistance of functionally graded materials. Acta Mater 52:4961–4972
Zhou YT, Lee KY (2011) Thermal response of a partially insulated interface crack in a graded coating-substrate structure under thermo-mechanical disturbance: Energy release and density. Theoret Appl Fract Mech 6:22–33
Zhou YT, Li X, Qin JQ (2007) Transient thermal stress analysis of orthotropic functionally graded materials with a crack. J Therm Stress 30:1211–1231
Zhou YT, Li X, Yu DH (2010) A partially insulated interface crack between a graded orthotropic coating and a homogeneous orthotropic substrate under heat flux supply. Int J Solids Struct 6:768–778